



Characteristics and temporal variations of organic and elemental carbon aerosols in a high-altitude, tropical Latin American megacity

Omar Ramírez^{a,b,*}, A.M. Sánchez de la Campa^{a,c}, Jesús de la Rosa^{a,c}

^a Associate Unit CSIC–University of Huelva “Atmospheric Pollution”, Centre of Research in Sustainable Chemistry–CIQSO, University of Huelva, Campus de El Carmen s/n, 21071 Huelva, Spain

^b Department of Civil and Environmental, Universidad de la Costa, Calle 58 #55–66, 080002 Barranquilla, Colombia

^c Department of Earth Sciences, University of Huelva, Campus de El Carmen s/n, 21071 Huelva, Spain



ARTICLE INFO

Keywords:

OC/EC
Carbonaceous aerosol
El Niño
PM₁₀
Megacity
Colombia

ABSTRACT

Bogota is a Latin American megacity located at an average altitude of 2600 m in the tropical Andes. It registers frequent episodes of poor air quality due to high PM₁₀ concentrations. The carbonaceous fraction is the main PM₁₀ component (> 50%), but there is a lack of specific studies analyzing the characteristics and temporal variability of organic carbon (OC) and elemental carbon (EC) aerosols. In this study, daily samples (24 ± 1 h) were collected from June 2015 to May 2016 (a total of 308 samples) at an urban background site during an El Niño year, and the quartz filters were analyzed using a thermal-optical method. Results showed that EC and organic matter accounted for ~60% of the PM₁₀ mass. The OC and EC averages were 8.92 ± 4.52 µg/m³ and 3.25 ± 1.59 µg/m³, respectively. The months with the highest average OC values were January to March, while EC concentrations were relatively constant throughout the year. Regarding daily values, the highest mean concentrations of OC (10.2 ± 5.13 µg/m³) and EC (3.73 ± 1.74 µg/m³) were obtained on Thursdays, and the lowest on Sundays (OC = 6.67 ± 3.04 µg/m³ and EC = 2.46 ± 0.94 µg/m³). The OC/EC ratio ranged from 1.66 (June) to 4.88 (March), with an annual average of 3.16 ± 2.01. The secondary organic carbon (SOC) contributions, measured using the EC-tracer method, accounted for 45% of the total OC. The effective carbon ratio, which indicates an association between carbonaceous particles and climate change, ranged from 0.12 (July) to 0.74 (May). The study of air-mass origins revealed that days with air mass from E + NE registered the highest OC concentrations. This research provides new data on the variability of carbonaceous aerosols over the course of a year. It also highlights forest fires as a significant source of OC and EC, and indicates the high impact of SOC on OC concentration at the sampling site.

1. Introduction

Atmospheric particulate matter with an aerodynamic diameter < 10 µm (PM₁₀) has been identified as one of the major urban air pollutants, particularly in developing cities (Gulia et al., 2015; UNEP, 2016). PM₁₀ is also considered a main risk factor for human health at a global scale (WHO, 2016; IHME, 2017). Several studies have revealed that the principal component of PM₁₀ in urban areas is the carbonaceous fraction (Querol et al., 2004; Fang et al., 2008), which has been linked to respiratory diseases, cardiac disorders, and infectious and allergic outcomes (Mauderly and Chow, 2008; WHO, 2012). Other research has reported the crucial role of carbonaceous particles in the deterioration of visibility, the formation of haze and clouds, atmospheric heating, and global climate change due to their light-absorption/scattering effects (Chung et al., 2012; Bisht et al., 2015; IPCC,

2015).

The carbonaceous fraction is generally classified into two main categories: elemental carbon (EC) and organic carbon (OC) (Castro et al., 1999). EC, a primary pollutant, is emitted during incomplete combustion of fossil fuels and biomass, and is considered as the main aerosol driving global warming (Jacobson, 2001; IPCC, 2015), and the second largest contributor to anthropogenic radiative forcing after CO₂ (Han et al., 2016). EC can be directly emitted into the atmosphere by natural and anthropogenic sources. In urban contexts anthropogenic sources prevail, making EC a good tracer of traffic, industry and biomass combustion emissions (Pio et al., 2011; Escudero et al., 2015). On the other hand, OC can increase Earth's reflectivity (Chameides and Bergin, 2002) and represents a mixture of thousands of organic compounds (such as polycyclic aromatic hydrocarbons – PAHs, polychlorinated biphenyls – PCBs, n-alkanes, among others) some of which represent

* Corresponding author.

E-mail addresses: oramirez@cuc.edu.co, omar.ramirez@unad.edu.co (O. Ramírez).

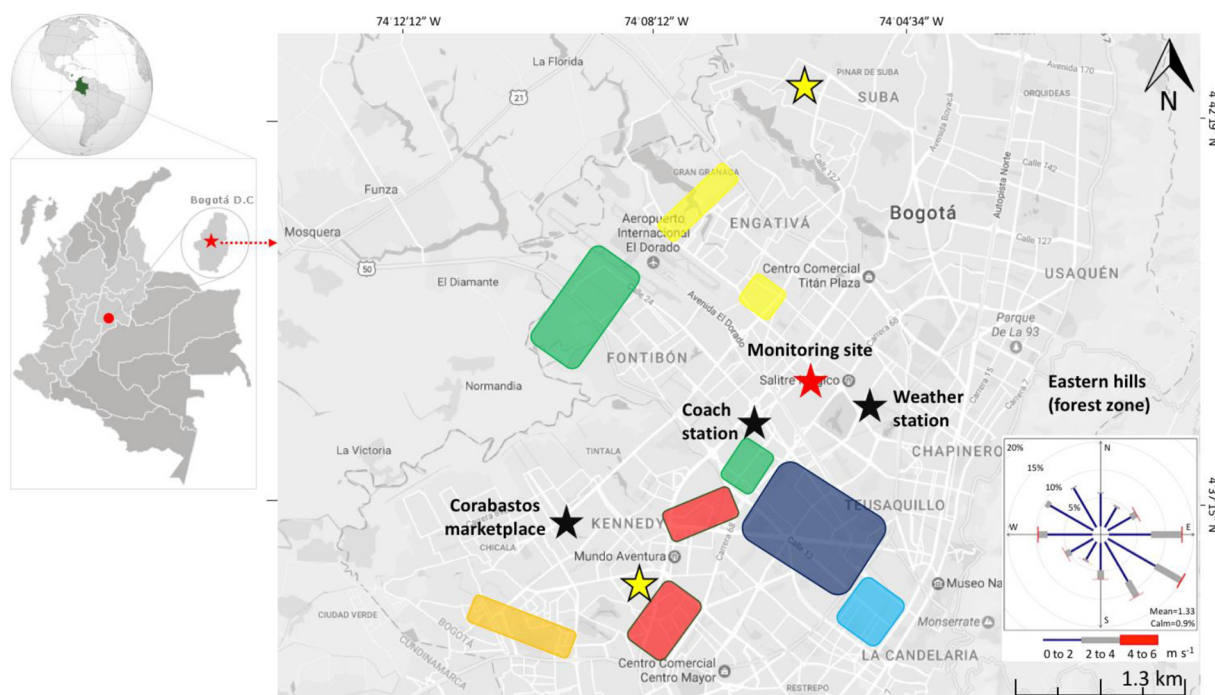


Fig. 1. Location of sampling point and weather station (Centro de Alto Rendimiento – CAR). Polygons indicate the main industrial zones near the sampling point, by color: yellow (Engativá), green (Fontibón), dark blue (Puente Aranda), red (Kennedy), orange (Bosa) and light blue (Los Mártires). All the zones have a diverse range of industrial activities, including food and beverages, chemicals (pesticides and other agricultural chemicals), textiles and the manufacture of metal and plastic products. Puente Aranda is notable for its concentration of metalworking facilities. Yellow stars indicate the sites sampled in previous studies (Vargas et al., 2012). The wind rose during the sampling period is shown. (For interpretation of the references to color in this figure legend, the reader is referred to the web version of this article.)

significant risks to human health (Mauderly and Chow, 2008; Feng et al., 2009). OC can either be emitted directly into the atmosphere (primary organic carbon – POC) from combustion processes and biogenic sources, or formed within the atmosphere (secondary organic carbon – SOC) through gas-to-particle conversion from volatile organic compounds (VOCs), either as a result of the condensation of low vapor pressure compounds or from physical/chemical adsorption of gaseous species on particle surfaces (Pandis et al., 1992; Fuzzi et al. 2006). SOC can also be formed by photochemical and thermal oxidation reactions of POC and organic gaseous carbon (Kroll and Seinfeld, 2008; Keller and Bartscher, 2017). As SOC represents up to 90% of OC, even in urban areas (Gelencsér et al., 2007), it is a good indicator of anthropogenic and natural VOCs.

Recent research has shown the importance of studying carbonaceous aerosols in the PM₁₀ fraction (Pipal and Satsangi, 2015; Godec et al., 2016; Wang et al., 2017), particularly in Latin American cities where urban pollution levels are high (Seguel et al., 2009; Green and Sánchez, 2013; Monteiro dos Santos et al., 2016; UNEP, 2016). One such case is Bogotá (the capital of Colombia), a Latin American megacity of over 8 million inhabitants (DANE, 2010) and one of the most densely populated tropical cities in the world (17,300 hab/km²) (Demographia, 2017), which is exposed to poor air quality (Molina et al., 2004a; Zhu et al., 2012; IDEAM, 2016; UNEP, 2016), including high values of carbonaceous aerosols (Vargas et al., 2012; Ramírez et al., 2018).

There are > 2 million private vehicles in Bogotá, with a further 460,000 motorcycles and > 50,000 taxis, as well as large numbers of buses and heavy-duty trucks. Most vehicular traffic (~95%) uses gasoline and only 5% (~90,000 vehicles) uses diesel (SDM, 2016). These mobile sources emit 1100–1300 tons of PM per year (Carmona et al., 2016). In addition to traffic, Bogotá has nearly 2000 industrial smokestacks (including the chemical industry, metallurgy, and petrochemical activities, among others) which emit about 1400 tons of PM

per year as a result of combustion processes (SDA, 2009). Consequently, PM₁₀ is the most significant pollutant affecting Bogotá's air quality (SDA, 2015, 2016). The carbonaceous fraction (EC + OM, organic matter) is the principal component of PM₁₀ (Vargas et al., 2012; Ramírez et al., 2018) and one of the main pollutants to which pedestrians and bike-path users are exposed (Segura and Franco, 2016; Franco et al., 2016). Despite this, there is a lack of research into the characteristics, origin and temporal variability of the carbonaceous aerosols. Preliminary analyses have characterized organic species in PM₁₀, such as PAH and n-alkanes (Vasconcellos et al., 2011). Other studies have measured the carbonaceous fraction concentration in ambient PM₁₀ from residential and industrial sites (Vargas et al., 2012). However, there are no detailed studies of the characteristics and temporal variations of OC and EC over a continuous year of sampling in Bogotá. The aim of this study is to expand the current knowledge of carbonaceous aerosols in this megacity over the course of a year characterized by the phenomenon known as El Niño Southern Oscillation (ENSO).

2. Materials and methods

2.1. Study area and PM₁₀ sampling

Bogotá (04°43' N; 74°04' W) is located at Eastern Range of the Andes (2550–2620 m above sea level) and has an area of ~1600 km². The average annual temperature and precipitation are 14 °C and 840 mm/year, respectively (IDEAM, 2015a). The months with the highest rainfall levels are April–May and October–November. Winds from NE–E and SE–E prevail with average speeds of 1.5–3.5 m/s and average maximum values of 10 m/s (IDEAM, 2015b).

Daily PM₁₀ samples were collected at 7:00 a.m. (24 ± 1 h) between 01 June 2015 and 31 May 2016, obtaining 308 filters in total. Hi-Vol Thermo Environmental Instruments Inc. and Hi-Vol Tisch

Table 1
Meteorological conditions during sampling period.

		Wind speed (m/s)	Temperature (°C)	RH (%)	Irradiance (W/m ²)	Precipitation (mm)
Whole period	Mean	1.32 ± 0.31	15.5 ± 1.00	65.4 ± 5.71	177 ± 51.2	52.5 ± 58.0
	Max	1.61	16.5	70.9	231	208
	Min	1.02	14.7	60.6	143	2.30
2015	Jun	1.54 ± 0.20	14.9 ± 0.71	66.1 ± 3.32	169 ± 28.8	24.8
	Jul	1.61 ± 0.30	14.9 ± 0.61	64.6 ± 4.25	176 ± 35.6	27.5
	Aug	1.52 ± 0.28	15.2 ± 0.66	62.4 ± 4.24	171 ± 42.1	23.5
	Sep	1.32 ± 0.26	15.1 ± 1.15	60.6 ± 4.94	189 ± 51.5	21.2
	Oct	1.21 ± 0.27	15.2 ± 0.76	64.5 ± 5.79	174 ± 35.9	80.7
	Nov	1.19 ± 0.23	15.5 ± 0.79	68.2 ± 6.62	163 ± 50.1	72.3
	Dec	1.47 ± 0.40	14.7 ± 0.96	61.8 ± 4.25	182 ± 55.4	2.30
	Jan	1.31 ± 0.20	15.8 ± 0.90	66.4 ± 3.68	231 ± 47.8	2.30
2016	Feb	1.28 ± 0.21	16.4 ± 0.91	63.3 ± 5.50	190 ± 62.2	11.0
	Mar	1.19 ± 0.21	16.5 ± 0.78	67.1 ± 4.61	192 ± 59.9	89.4
	Apr	1.02 ± 0.26	15.8 ± 0.98	70.9 ± 7.11	143 ± 42.9	208
	May	1.22 ± 0.35	15.6 ± 0.83	68.5 ± 4.52	147 ± 41.3	67.2

Environmental Inc. samplers were used, which were located 3 m from ground level. The equipment was calibrated monthly to guarantee quality of the measurements. Hi-Vol flow rate was $1.13 \pm 0.18 \text{ m}^3/\text{min}$, and MK 360 ($203 \times 254 \text{ mm}$) quartz fiber filters pre-combusted and pre-conditioned for 4 days ($T = 20 \pm 1^\circ\text{C}$ and $\text{RH} = 50 \pm 5\%$) were used. All filters were gravimetrically analyzed before and after sampling with a $\pm 0.001 \text{ mg}$ microbalance to determine the amount of PM. PM_{10} concentrations were corrected to standard conditions (760 mmHg and 25°C) (US EPA, 1999), taking into consideration atmospheric pressure and local temperature. The procedure suggested by Bravo et al. (2013) was applied. The sampling site was located at the Universidad Libre campus ($04^\circ39'52.87'' \text{ N}$; $74^\circ06'07.26'' \text{ W}$) (Fig. 1). This site is considered an urban background area because it is surrounded by green areas and has no direct influence from emission sources (the nearest street with traffic is at $> 400 \text{ m}$ and the closest industrial area is $> 2 \text{ km}$).

The ranges of wind speed, temperature, relative humidity, irradiance and precipitation were $1.0\text{--}1.6 \text{ m/s}$, $15\text{--}17^\circ\text{C}$, $61\text{--}71\%$, $143\text{--}231 \text{ W/m}^2$ and $2.3\text{--}208 \text{ mm}$ respectively during the sampling period (Table 1). The ENSO phenomenon was present during the year of sampling, meaning that precipitation levels were lower than the historic data for the location (SDA, 2017, 2016). Hourly means of wind direction frequency and wind speed are plotted in Supplementary Fig. 1. Meteorological data were taken from the CAR (Centro de Alto Rendimiento) air quality station located approximately 1.5 km from the sampling point (Fig. 1).

2.2. Chemical characterization

After PM_{10} gravimetric analysis, a 1.5 cm^2 rectangular portion of each quartz filter was analyzed for OC, EC and Total Carbon (TC, with $\text{TC} = \text{OC} + \text{EC}$) by a Thermal Optical Transmittance (TOT) method (Birch and Cary, 1996) using a carbon analyzer (Sunset Laboratory Inc.) at the University of Huelva. The EUSAAR2 (European Supersites for Atmospheric Aerosol Research) protocol was followed (Cavalli et al., 2010). In this analysis, the carbonaceous material was exposed to different thermal conditions, so that the samples were thermally desorbed from the filter medium under an oxygen-free inert helium atmosphere (200°C to 650°C), followed by an oxidizing atmosphere containing an oxygen/helium mixture (500°C to 850°C) (Supplementary Table 1). OC was vaporized in an inert atmosphere in the first step, while EC was converted into vapor upon exposure to higher temperature and an oxidation atmosphere ($98\% \text{ He}$ and $2\% \text{ O}_2$) in the second step.

As some organic compounds can be readily pyrolyzed in the first step, the equipment continuously monitored the optical properties of the sample (reflectance and transmittance) and automatically corrected the values to avoid incorrect reports. A manganese dioxide catalyst

converted the liberated carbon compounds into carbon dioxide, which was reduced to methane to calculate the concentrations of OC and EC. Discrimination between OC and EC was achieved by monitoring the transmission of laser light through the filter.

Quality control was implemented through use of an external sucrose aqueous solution which ensured the consistent operation of the instrument and the quality of the measurements. The detection limit for TC was calculated from values of ten white filters. It was $0.4 \mu\text{g}/\text{cm}^2$ per section of filter. Precision and accuracy of the TOT technique were lower than 5% and were evaluated after repeated analysis of standards (sucrose 99.9% reagent grade) of known concentration ($42.1 \mu\text{g}/\text{cm}^2$). All values of the concentrations were corrected from white filter values.

2.3. Estimation of secondary organic carbon (SOC)

OC/EC ratios higher than 2.0 indicate possible SOC formation (Chow et al., 1996). Since it is not possible to obtain direct SOC measurements due to the complex physical and chemical processes involved, an indirect method was used. The method applied to estimate SOC concentrations was the EC-tracer method, based on minimum OC/EC ratios. This method uses EC as a tracer for primary OC and assumes that EC (unlike POC) is unaffected by photochemical oxidation reactions and the ratio of primary OC/EC remains constant throughout the whole campaign (Castro et al., 1999). SOC was calculated using the following equation:

$$\text{SOC} = \text{OC}_{\text{total}} - \left(\frac{\text{OC}}{\text{EC}} \right)_{\text{min}} \times \text{EC} \quad (1)$$

where SOC is secondary organic carbon, and OC_{total} and EC are the respective environmental concentrations. This study selected the 5th percentile of the OC/EC ratio as $(\text{OC}/\text{EC})_{\text{min}}$ as this is considered the most adequate to avoid atypical values (Pio et al., 2011; Khan et al., 2016; Monteiro dos Santos et al., 2016; Ji et al., 2016). The $(\text{OC}/\text{EC})_{\text{min}}$ ratios were representative of the primary carbon level in the sampled atmosphere (Pio et al., 2011). Considering that the ambient temperature was relatively constant during the sampling period (Table 1), possible changes in semi-volatile sampling efficiency were considered negligible. Some limitations of the OC/EC minimum ratio method, such as disregarding the variability of primary sources and not considering non-combustion OC associated with EC, have been discussed in other studies (Khan et al., 2016).

The concentration of organic matter (OM) was obtained by multiplying OC data by a factor of 2.1, taking into consideration the site conditions and the recommendations for aerosols in urban areas impacted by different emission sources (Chen and Yu, 2007; El-Zanani et al., 2009).

Table 2

Descriptive statistics for PM₁₀ mass, EC, OC, OM and TC at the study site, stating the mean and standard deviation (SD) of concentrations for each month. All concentrations are in $\mu\text{g}/\text{m}^3$; OC/EC ratio is in $\mu\text{g}/\mu\text{g}$. All data are recorded in the form: mean \pm SD.

Whole year	(N = 308)	PM ₁₀	EC	OC	TC	OM	OC/EC
		37.5 \pm 21.5	3.25 \pm 1.59	8.92 \pm 4.52	12.2 \pm 5.20	18.7 \pm 9.49	3.16 \pm 2.01
2015	Jun (N = 22)	29.6 \pm 28.0	2.81 \pm 0.99	4.66 \pm 1.94	7.48 \pm 2.80	9.79 \pm 4.08	1.66 \pm 0.44
	Jul (N = 28)	22.9 \pm 6.65	3.10 \pm 1.10	5.71 \pm 1.93	8.81 \pm 2.98	12.0 \pm 4.05	1.89 \pm 0.27
	Aug (N = 28)	21.4 \pm 8.29	3.13 \pm 1.96	5.22 \pm 2.08	8.34 \pm 3.48	11.0 \pm 4.36	1.94 \pm 0.75
	Sep (N = 29)	25.8 \pm 10.2	3.00 \pm 1.25	7.37 \pm 3.53	10.4 \pm 3.99	15.5 \pm 7.42	2.76 \pm 1.42
	Oct (N = 28)	34.2 \pm 16.9	3.23 \pm 1.45	8.99 \pm 3.60	12.2 \pm 3.98	18.9 \pm 7.56	3.27 \pm 1.90
	Nov (N = 29)	38.6 \pm 14.7	4.03 \pm 2.01	9.29 \pm 4.00	13.3 \pm 5.08	19.5 \pm 8.40	2.57 \pm 1.28
2016	Dec (N = 19)	29.2 \pm 10.1	2.73 \pm 1.51	7.42 \pm 3.01	10.3 \pm 3.73	15.6 \pm 6.33	3.43 \pm 1.81
	Jan (N = 23)	66.7 \pm 29.0	4.12 \pm 2.26	12.5 \pm 4.36	16.6 \pm 5.65	26.2 \pm 9.17	3.50 \pm 1.53
	Feb (N = 26)	50.7 \pm 17.7	3.02 \pm 1.23	11.8 \pm 4.93	14.8 \pm 5.53	24.8 \pm 10.3	4.35 \pm 2.12
	Mar (N = 28)	59.7 \pm 18.8	3.06 \pm 1.12	13.6 \pm 3.92	16.7 \pm 4.41	28.7 \pm 8.22	4.88 \pm 1.91
	Apr (N = 23)	44.2 \pm 14.2	3.61 \pm 1.55	11.5 \pm 4.26	15.2 \pm 4.53	24.3 \pm 8.95	3.96 \pm 2.91
	May (N = 25)	29.7 \pm 11.0	3.10 \pm 1.73	8.80 \pm 3.78	11.9 \pm 4.27	18.5 \pm 7.94	3.84 \pm 2.95

2.4. Study of air masses

In order to analyze the potential effects of long-range transports on the concentrations of carbonaceous aerosols, air mass back trajectories were calculated using the National Oceanic and Atmospheric Administration (NOAA) HYSPLIT v. 4 model (<http://ready.arl.noaa.gov/HYSPLIT.php>) (Stein et al., 2015; Rolph et al., 2017), with GDAS meteorological information (0.5°). Since regional anthropogenic secondary organic aerosols are formed within a timescale of approximately one day (DeCarlo et al., 2010) and their lifetime has been estimated to be 4–5 days (Molina et al., 2004b), daily back trajectories were plotted during the sampling period with a run time of 72 h, calculated every six hours, at 12:00 UTC, at an arrival height within the mixing-layer (500 m above ground level).

3. Results and discussion

3.1. PM₁₀ and levels of carbonaceous species

Table 2 summarizes the descriptive statistics for the PM₁₀ mass, EC and OC concentrations at the sampling site, while mean values are plotted in Fig. 2. During the sampling campaign, PM₁₀ levels were in the range 9.89 $\mu\text{g}/\text{m}^3$ (06/01/2015)–160 $\mu\text{g}/\text{m}^3$ (01/20/2016) (mean 37.5 \pm 21.5 $\mu\text{g}/\text{m}^3$). The results showed that PM₁₀ was almost twice as high as the World Health Organization (WHO) guidelines (20 $\mu\text{g}/\text{m}^3$ annual mean) (WHO, 2006).

OC values ranged from 2.17 $\mu\text{g}/\text{m}^3$ to 24.5 $\mu\text{g}/\text{m}^3$, and EC values from 0.69 $\mu\text{g}/\text{m}^3$ to 11.3 $\mu\text{g}/\text{m}^3$. The OC and EC averages were 8.92 \pm 4.52 $\mu\text{g}/\text{m}^3$ and 3.25 \pm 1.59 $\mu\text{g}/\text{m}^3$, respectively. These concentrations were similar to those previously reported at a residential site in Bogota (7.55 and 4.55 $\mu\text{g}/\text{m}^3$, respectively, $n = 55$), but lower than those found in an industrial zone in the same city (11.85 and 6.77 $\mu\text{g}/\text{m}^3$, respectively, $n = 56$) (Vargas et al., 2012).

The mean OC concentrations in the present study were comparable to those reported in high-traffic urban areas (Budapest, Lisbon and Thessaloniki), and urban/rural zones with industrial influence in Thessaloniki and Delnice (Table 3). The OC results were three times those reported in urban background sites in Lisbon and Sao Paulo, and up to twice as high as those found in urban areas in London, Birmingham, Aragón and Ghent. However, OC concentrations were lower than those in large cities such as Santiago de Chile, Mexico City, Zhengzhou, Kaohsiung, Pune and Baotou (Table 3).

EC concentrations were in the range of values reported in residential/background sites (London and Lisbon in winter time), high traffic avenues (Budapest, Mexico City and Sao Paulo), and industrial areas (Thessaloniki and Pune). They were higher than those in several urban backgrounds in European and British cities (e.g. Aragón, Prague,

Zagreb, Birmingham and Lisbon in summer time), but were significantly lower than levels at urban sites in densely-populated cities such as Santiago de Chile, Zhengzhou, Baotou and Kaohsiung (Table 3).

3.2. Temporal variations and origin of OC and EC

The OC values oscillated synchronously with PM₁₀ concentrations ($R^2 = 0.77$). January, February and March were the months with the highest average OC values (12.5 \pm 4.36 $\mu\text{g}/\text{m}^3$, 11.8 \pm 4.93 $\mu\text{g}/\text{m}^3$ and 13.6 \pm 3.92 $\mu\text{g}/\text{m}^3$, respectively) (Table 2). This period recorded the most significant peaks in OC concentration, as a result of large forest fires in Bogota (SDA, 2017) caused by high temperatures (Fig. 2). Open biomass burning, including forest fires, has been linked to elevated OC concentrations (Zhang et al., 2008; Wang et al., 2017).

The sampled area was influenced by El Niño phenomenon at synoptic level during the study period. This is observed by analyzing the Oceanic Niño Index (ONI) data (Supplementary Table 2). In Bogota, El Niño reduces the levels of precipitation and increases the temperature (IDEAM, 2014). Thus, El Niño year was drier and warmer than normal years (Supplementary Tables 3 and 4), with December, January and February being the most affected months, during which the main forest fires in Bogota and surrounding regions were recorded. This suggests that El Niño indirectly affected the concentrations of carbon aerosols by accentuating the conditions of the dry season (low rainfall and high temperatures), promoting forest fires (Supplementary Figs. 2 and 3).

The wind rose for January and February shows the predominance of winds from SE–E–NE (~50%) (Supplementary Fig. 1), where the Eastern Hills were located (Fig. 1). Observations of the polar plots revealed that the highest concentrations of OC were in the same direction (SE) at wind speeds between 1.2 m/s and 1.5 m/s (Figs. 3A and B). This indicates that the forest fires had a large impact on OC concentrations. A different pattern was recorded in March, when the dominant winds came from NW–W–SW (> 50%) (Supplementary Fig. 1). In this period, the highest concentrations of OC were registered when the wind blew from W–SW–S (Fig. 3C) at low wind speeds (< 1.6 m/s). This suggests that during March, high OC concentrations had an anthropogenic origin, emitted by local sources such as traffic and industrial activities located in the west and south of the city in the localities of Fontibón, Kennedy, Bosa and Puente Aranda (Fig. 1). Puente Aranda is of particular significance because of its proximity to the sampling point (~2.5 km) and because it brings together the largest number of industries in Bogota (SDA, 2009). On the other hand, the lowest concentrations of OC were recorded in June, July and August (4.66 $\mu\text{g}/\text{m}^3$, 5.71 $\mu\text{g}/\text{m}^3$ and 5.22 $\mu\text{g}/\text{m}^3$, respectively) (Table 2), when the highest monthly wind speeds (Table 1) and the maximum daily values (> 2.2 m/s in July 03 and 04) were reported, facilitating air pollutant dispersion. Overall, the data show significant variation in OC

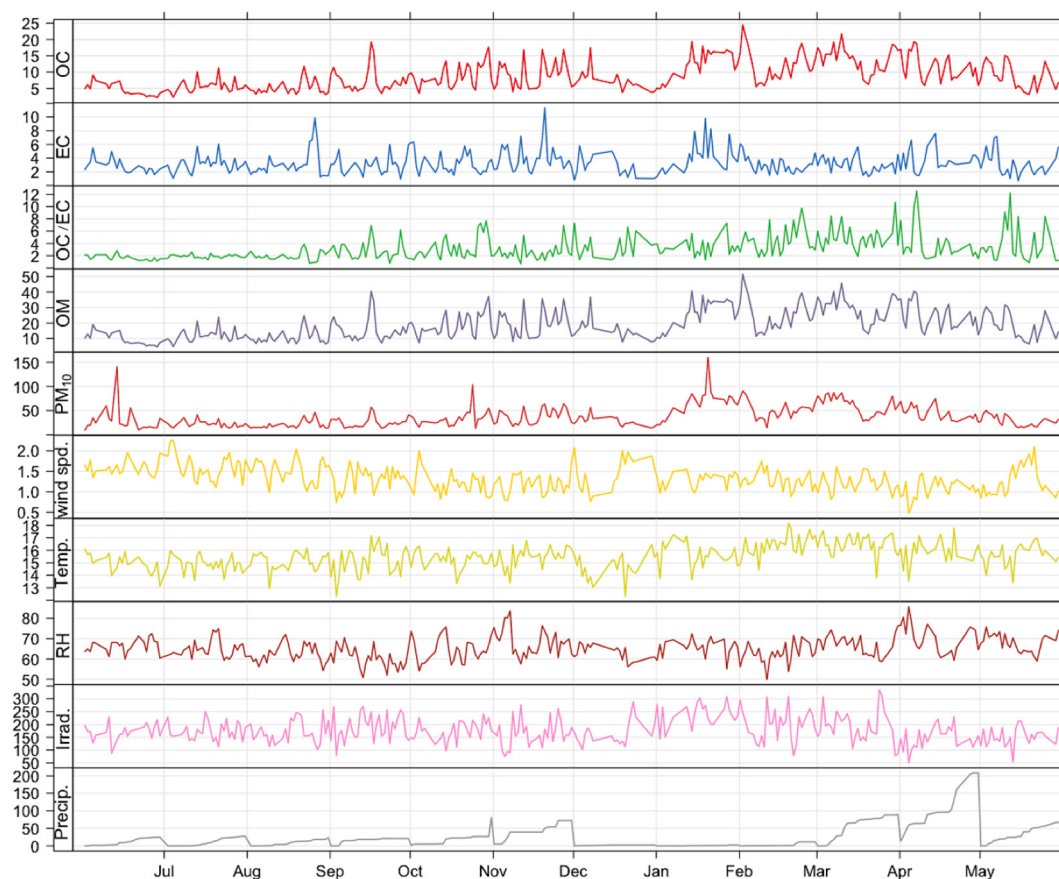


Fig. 2. Monthly variation of carbonaceous species, PM_{10} ($\mu\text{g}/\text{m}^3$) and meteorological parameters in Bogotá: wind speed (m/s), Temperature ($^{\circ}\text{C}$), RH (%), Irradiance (W/m^2) and precipitation (accumulated mm/month).

Table 3

Average concentrations of OC, EC and OC/EC ratios in different cities.

Site	Location	N	Concentrations ($\mu\text{g}/\text{m}^3$)			OC/EC	Protocol	References
			PM_{10}	EC	OC			
Urban background	Bogota, Colombia	308	37.5	3.25	8.92	3.16	EUSAAR2	This study
Urban background	Zagreb, Croatia	121	19.4–43.6	0.6–1.6	5.0–12.0	8.5–9.2	NIOSH	Godec et al., 2016
Urban background	Aragón, Spain	47	32	0.6	4.9	14.2	NIOSH	Escudero et al., 2015
Urban background	Huelva, Spain	46	39	1.5	3.5	2.3	Uninformed	Sánchez De La Campa et al., 2009
Urban background	London, UK	151	23.15	2.55	5.17	2.03 ^a	Uninformed	Harrison et al., 2004
Urban background	Birmingham, UK	–	23.9	1.8	3.8	2.1	Uninformed	Yin and Harrison, 2008
Urban background	Prague, Czech Republic	137	33	0.74	5.5	8.0	NIOSH	Schwarz et al., 2008
Urban background	Lisbon, Portugal	48	24–26	1.2–3.0	2.7–3.3	1.0–2.2	Uninformed	Alves et al., 2016
Urban background	Hong Kong, China	70	80	1.48	5.62	3.79 ^b	Uninformed	Ho et al., 2003
Residential	Bogota, Colombia	55	41.4	4.55	7.55	1.66	NIOSH	Vargas et al., 2012
Park	Sao Paulo, Brazil	28	27	1.50	2.65	1.89	EUSAAR2	Monteiro dos Santos et al., 2016
Urban	Ghent, Belgium	24	20.0	1.0	3.5	3.5 ^a	Uninformed	Viana et al., 2006
Urban	Mexico City, Mexico	28	74–95	4.4–5.3	14–17	3.15 ^a	NIOSH	Mugica et al., 2009
Urban	Kaohsiung, Taiwan	102	111	6.1	14.5	2.4 ^a	Uninformed	Lin and Tai, 2001
Urban	Santiago de Chile, Chile	9	250	30.6	54.2	1.7 ^a	Uninformed	Didyk et al., 2000
Urban	Zhengzhou, China	53	214	13	34	3.2	NIOSH	Wang et al., 2017
Traffic	Sao Paulo, Brazil	41	35	2.25	3.24	1.57	EUSAAR2	Monteiro dos Santos et al., 2016
Traffic	Lisbon, Portugal	48	41–48	6.0–7.4	5.5–6.8	0.9–1.0	Uninformed	Alves et al., 2016
Traffic	Budapest, Hungary	23	21–107	0.9–10	4.6–24	1.1–2.9	Uninformed	Salma et al., 2004
Traffic	Thessaloniki, Greece	78	42–51	1.82–2.64	7.66–8.07	2.90–4.43	Uninformed	Terzi et al., 2010
Traffic	Aragón, Spain	86	25	1.2	4.0	4.7	NIOSH	Escudero et al., 2015
Industrial	Pune, India	–	170	2.40	33.14	17.2	NIOSH	Pipal and Satsangi, 2015
Industrial	Baotou, China	402	176	7.7	21.8	2.8	IMPROVE	Zhou et al., 2016
Industrial	Thessaloniki, Greece	81	58–69	2.91–2.93	6.40–8.73	2.20–2.98	Uninformed	Terzi et al., 2010
Industrial	Bogota, Colombia	56	52.0	6.77	11.8	1.74	NIOSH	Vargas et al., 2012
Rural industrial	Delnice, Croatia	121	19.3–47.0	0.5–2.2	5.8–18.9	10.7–14.0	NIOSH	Godec et al., 2016

^a Values not reported in original paper but calculated for this work based on the OC and EC values. NIOSH = National Institute for Occupational Safety and Health. IMPROVE = Interagency Monitoring of Protected Visual Environment. EUSAAR = European Supersites for Atmospheric Aerosol Research.

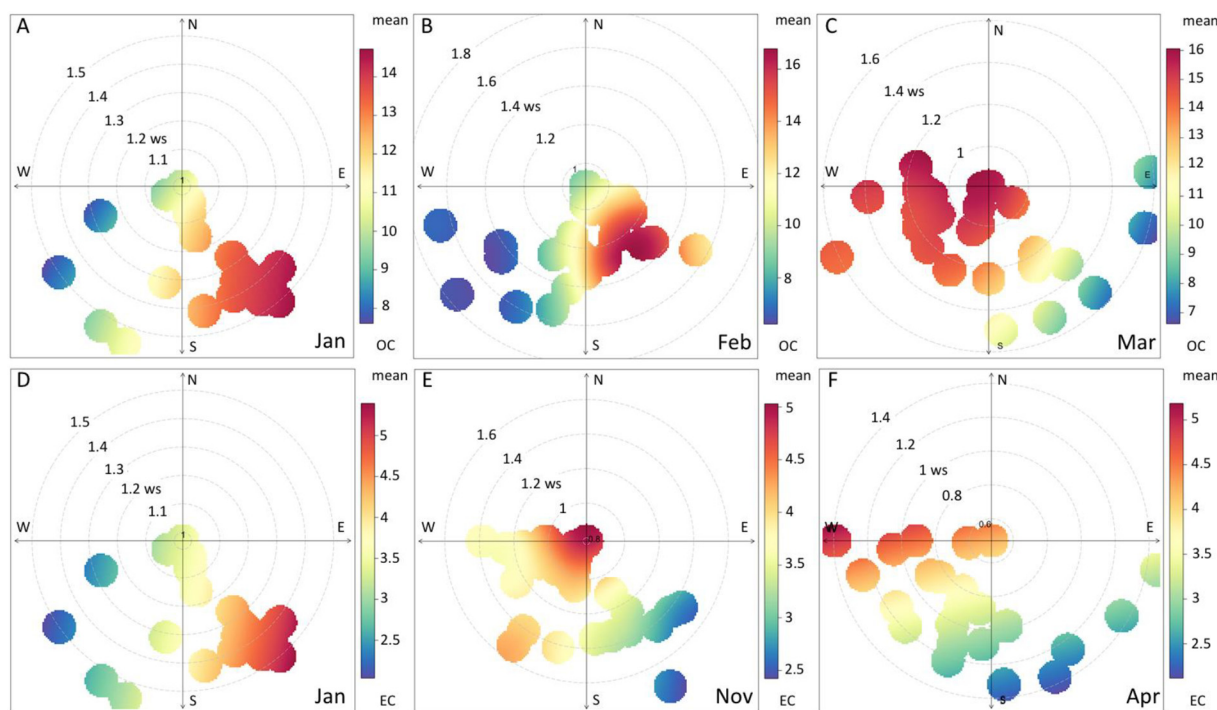


Fig. 3. Polar plot of the months with the highest concentrations of OC (A, B and C) and EC (D, E and F).

concentrations over the year, with the figure for the month with the highest mean concentration (March) three times that of the month with the lowest (June).

By contrast, EC concentrations were relatively constant throughout the year of sampling. In this case, the figure for the month with the highest mean concentration (January, $4.12 \pm 2.26 \mu\text{g}/\text{m}^3$) is somewhat less than twice that of the month with the lowest concentration (December, $2.73 \pm 1.51 \mu\text{g}/\text{m}^3$) (Table 2). January, November and April ($4.12 \pm 2.26 \mu\text{g}/\text{m}^3$, $4.03 \pm 2.01 \mu\text{g}/\text{m}^3$ and $3.61 \pm 1.55 \mu\text{g}/\text{m}^3$, respectively) were the months with the highest concentrations of EC.

Analyzing the wind rose (Supplementary Fig. 1) and polar plots for EC in January (Fig. 3D), it can be seen that the prevailing winds came from SE–E–NE (~50%), where forest fires occurred in the Eastern Hills. This suggests that the forest fires had a significant impact on the EC concentration, which is consistent with other studies that have linked the occurrence of these events to an increase in EC concentrations (Gelencsér et al., 2007; De Oliveira et al., 2015). The prevailing winds during November and April (Supplementary Fig. 1) came from W and the highest concentrations of EC were obtained from W–SW (Figs. 3E and F). This indicates the high influence of industrial combustion at locations in Fontibón, Kennedy and Puente Aranda. Other EC sources to consider are the city's main coach station (mobilizing about 1,200,000 diesel coach journeys per year) and the largest supply market in Bogotá, “Corabastos” (served by > 5 thousand diesel trucks a day), both of which are located to the SW of the sampling site at ~2 km and ~7 km, respectively. It is also worth mentioning that there are ~90,000 diesel vehicles circulating around the city (SDM, 2016). Diesel vehicles in Bogotá usually have high EC emissions (SDA, 2009) due to delays in implementing emission control legislation.

Months with high rainfall levels (November and April) registered high concentrations of EC, which could be accounted for by the unfavorable dispersion conditions for atmospheric pollutants, including low wind speeds (Table 1) and low boundary layer height. These are typical meteorological conditions during the rainy season (Lonati et al., 2007; Zhou et al., 2016; Ramírez et al., 2018). Considering that the majority of EC mass (~80%) is in the fine mode (Hitzenberger et al.,

2006; Huang and Yu, 2008), it is expected that the scavenging rates of these carbonaceous species will be low. This is due to the theory of collision efficiency between particles and rain droplets (Slinn, 1984), where it has been reported that the wet scavenging coefficient of fine particles is quite poor (Guo et al., 2016). The increase in EC levels can be explained by the fact that local emissions (especially traffic) rise and the dispersion conditions are not favorable during the rainy months, in such a way that the EC contribution is higher than the wet sweep rate caused by the raindrops. This effect has been reported in other studies (Feng and Wang, 2012; Yuan, 2014). Another possible reason for the increase in elemental carbon is the dominance of EC particles freshly emitted by combustion processes, since these present hydrophobic properties when they are recently emitted (Tritscher et al., 2011; Custódio et al., 2014). This condition decreases the scavenging rates. The above suggests that the EC measured at the sampling site comes predominantly from nearby emission sources, such as traffic, during the rainy months. January was an exceptional month as it presented low levels of precipitation, but high concentrations of EC, confirming the impact of forest fires as a source of EC through byproducts of incomplete combustion.

June, September and December recorded the lowest EC concentrations ($2.81 \mu\text{g}/\text{m}^3$, $3.00 \mu\text{g}/\text{m}^3$ and $2.73 \mu\text{g}/\text{m}^3$, respectively). During these months, winds came mainly from E–SE, reaffirming the idea that the EC concentration was higher when contaminated air masses arrived at the sampling site from the NW–W–SW of the city, including industrial parks of municipalities located to the west of Bogotá like Mosquera and Funza (Fig. 1).

Fig. 4 shows the variations in concentrations of OC and EC according to the days of the week. The highest mean concentrations of OC ($10.2 \pm 5.13 \mu\text{g}/\text{m}^3$) and EC ($3.73 \pm 1.74 \mu\text{g}/\text{m}^3$) were obtained on Thursdays, and the lowest (OC = $6.67 \pm 3.04 \mu\text{g}/\text{m}^3$ and EC = $2.46 \pm 0.94 \mu\text{g}/\text{m}^3$) on Sundays (Fig. 4A). These figures represent a significant difference in mean OC and EC concentrations (of 54% and 52%, respectively) on Thursdays in comparison with Sundays. OC and EC concentrations were lower on the weekends ($7.05 \pm 0.54 \mu\text{g}/\text{m}^3$ and $2.60 \pm 0.20 \mu\text{g}/\text{m}^3$, respectively) compared to weekdays ($9.62 \pm 0.48 \mu\text{g}/\text{m}^3$ and $3.51 \pm 0.16 \mu\text{g}/\text{m}^3$,

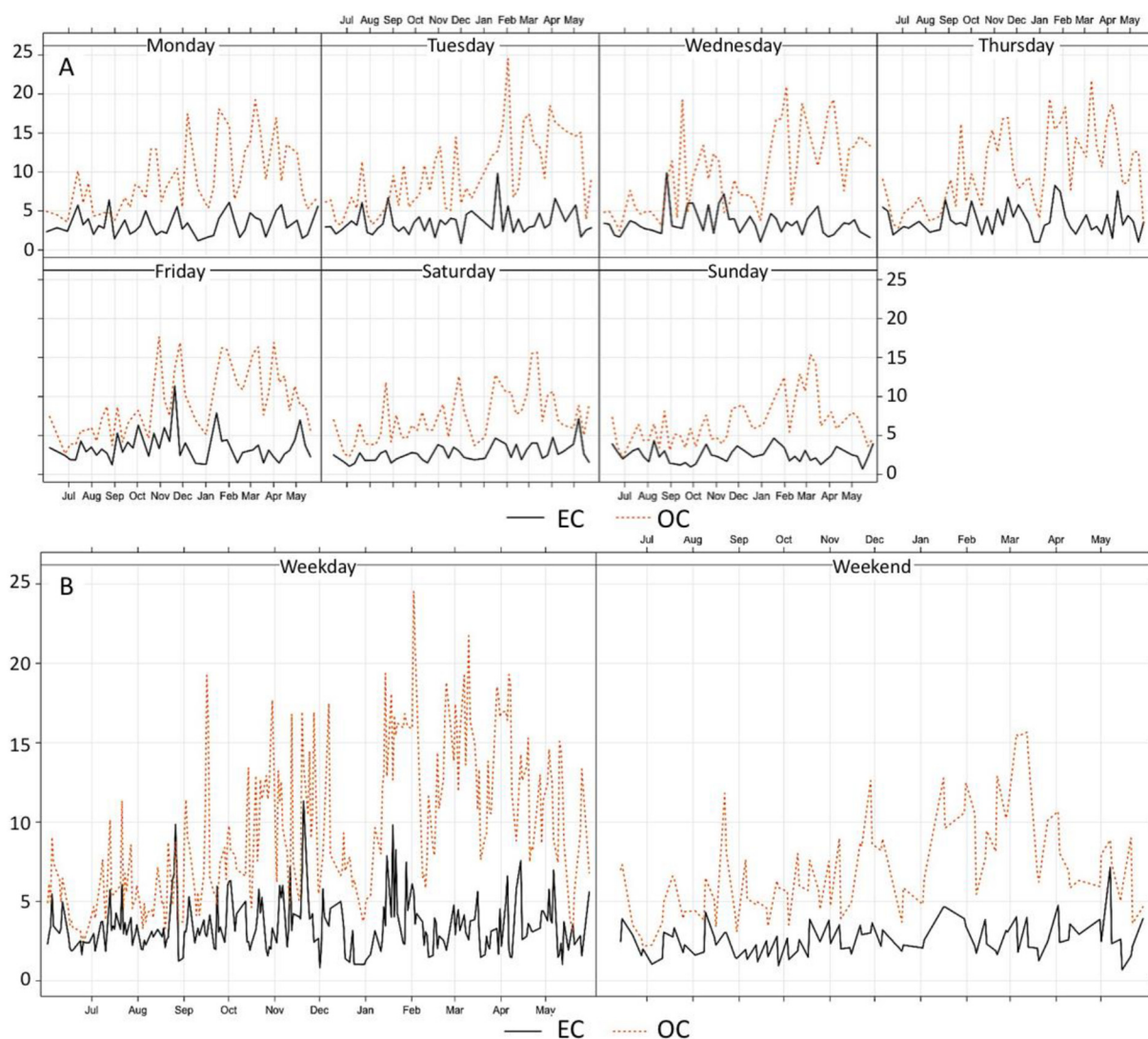


Fig. 4. Descriptive statistics for daily variation in OC and EC ($\mu\text{g}/\text{m}^3$): A) concentrations for individual days during the sampling period, B) average concentrations for weekdays as opposed to weekends.

respectively) (Fig. 4B), representing an overall increase in the concentration of carbonaceous aerosols on weekdays of $\sim 35\%$ in comparison with weekends. This is consistent with what has been reported in other urban sites (Grivas et al., 2012), but does not coincide with results found in other megacities such as Beijing, where OC and EC concentrations are slightly higher on the weekends (Ji et al., 2016). This suggests higher anthropogenic activities on working days.

3.3. Contribution of carbonaceous aerosol to PM_{10}

TC concentration (OC + EC) accounted for $\sim 33\%$ of PM_{10} ($12 \mu\text{g}/\text{m}^3$). This result resembles previous reports from other urban areas in Bogota (29%, Vargas et al., 2012) and urban background sites in London (33%, Harrison et al., 2004) and Zagreb during winter time (31%, Godec et al., 2016). The percentage obtained was slightly higher than that of urban areas in Beijing (25%, Duan et al., 2005), Zhengzhou (22%, Wang et al., 2017) and Ghent (22%, Viana et al., 2006). It was higher than data from a traffic zone in Sao Paulo (16%, Monteiro dos Santos et al., 2016), an industrial area in Baotou (17%, Zhou et al., 2016), and an urban background in Hong Kong (8.9%, Ho et al., 2003).

EC alone accounted for 8.7% of PM_{10} ($3.2 \mu\text{g}/\text{m}^3$). This percentage was higher during July and August (13% and 15%, respectively), when the highest wind speeds were reported (Table 1). The lowest percentage

was obtained in March (5.1%). Meanwhile, OC alone accounted 24% for PM_{10} ($8.9 \mu\text{g}/\text{m}^3$), reaching its highest values in May and September (30% and 29%, respectively) and the lowest in June (16%).

The mean value of OM accounted for 50% ($19 \mu\text{g}/\text{m}^3$) of PM_{10} mass and was similar to measurements obtained by previous studies in Bogota (43%, Vargas et al., 2012; 42%, Ramírez et al., 2018). The results were slightly higher than those reported in an urban background site in Los Angeles (20%–40%, Chow et al., 1994) and Dar es Salaam (37%, Mkoma et al., 2009), and were twice the level of an urban background in London (20.9%, Harrison et al., 2004) and Hong Kong ($\sim 20\%$, Ho et al., 2003). Monthly average contributions of OM to PM_{10} were calculated and it was observed that May registered the highest percentage (62%) and June the lowest (33%). The reasons for this monthly variability were not clear, although factors could include the temporary domain of primary and secondary sources of organic aerosols, variability in the degree of aging of OM as a function of the contribution of non-oxygen elements (Philip et al., 2014), the meteorological variables that condition the formation of OC from gas-to-particle conversion processes, the concentration of primary organic aerosols and fresh SOC which alter the OM/OC ratio (Aiken et al., 2008), and regional and long range transport of organic aerosols at different times of the year.

The considered OM/OC ratio (2.1) could vary according to the

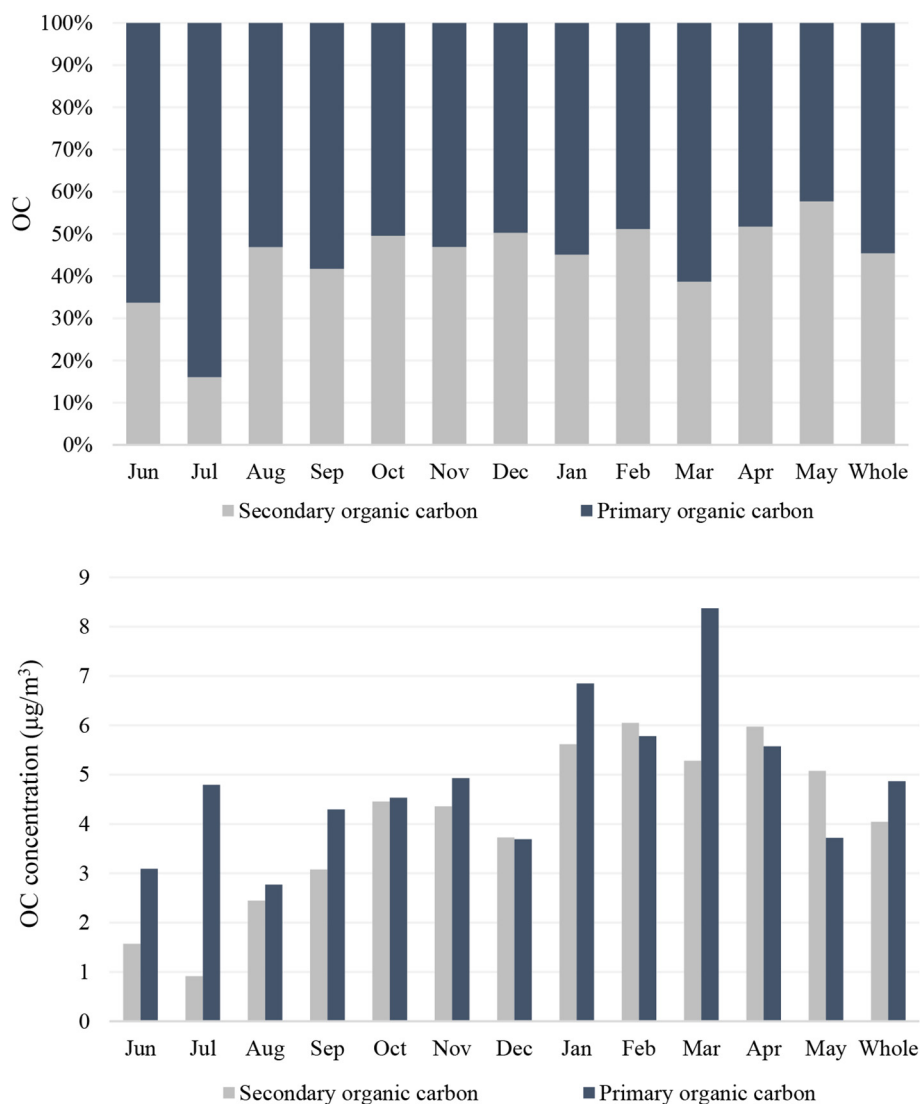


Fig. 5. Contribution (%) and mean monthly concentration ($\mu\text{g}/\text{m}^3$) of SOC and POC.

influence of the sources, since groups of organic compounds were emitted from a variety of sources (such as industrial processes, vehicular traffic, biomass burning and biogenic emissions), and they did not maintain the same intensity throughout the year. In this way, it is possible that the contributions of OM to PM_{10} levels were undervalued in forest fires events, for example, or overvalued in periods with optimal weather conditions for the dispersion of local emissions. More specific research in this field should be carried out.

3.4. The OC/EC ratio

As shown in Table 2, the OC/EC ratio ranged from 1.66 (June) to 4.88 (March). The annual average was 3.16 ± 2.01 , which was double the ratio in other residential areas of the city with high vehicular traffic and industrial influence (Vargas et al., 2012). This figure was comparable to findings in urban areas in megacities such as Mexico City (Mugica et al., 2009), Hong Kong (Ho et al., 2003) and Beijing (Duan et al., 2005). It was less than the data reported for Chinese cities such as Fuzhou (Xu et al., 2012), but exceeded the ranges reported in some European cities such as Lisbon and Budapest (Alves et al., 2016; Salma et al., 2004).

Usually, high OC/EC ratios are systematically linked to low EC concentrations, and low ratios to high EC values (Novakov et al., 2005). However, the results from this study indicate a rather different pattern

in which OC/EC ratios are chiefly linked to variations in OC concentrations. A close look at the monthly averages of EC shows little variation during the study period ($2.73 \mu\text{g}/\text{m}^3 - 4.12 \mu\text{g}/\text{m}^3$) (Table 2), whereas there is a significant correlation between OC and OC/EC ratios ($R^2 = 0.79$) in the same period (Supplementary Fig. 4). Consequently, the highest values of the OC/EC ratio were measured in February and March (OC/EC > 4), when forest fires were occurring in Bogota and surrounding municipalities (SDA, 2017). These high values are consistent with previous studies, which have linked emissions from biomass burning with high OC/EC ratios (Samara et al., 2014; Wang et al., 2017) and SOC formation in addition to primary OC (Na et al., 2004).

The data suggest that the origin of the carbonaceous fraction was dominated by primary sources, such as industrial emissions and vehicle exhaust during June, July and August. These months recorded OC/EC ratios between 1.5 and 2 (Table 2). Previous studies have related values of OC/EC ~ 1.5 with light duty vehicles (Pio et al., 2011; Brito et al., 2013), which corresponds to the conditions in Bogota, where 95% of vehicular traffic uses gasoline. The correlation coefficient (R^2) between OC and EC was 0.63 in June and 0.86 in July (Supplementary Fig. 5), indicating the existence of a common source, such as traffic emissions.

On the premise that EC is mainly a primary pollutant from incomplete combustion emissions such as industrial coal consumption, biomass burning and traffic, values of OC/EC > 2 have been used as an indicator of SOC formation (Chow et al., 1994; Wu et al., 2013). The

high OC/EC ratios registered in this study strongly suggest that during most of the sampling year (with the exception of June, July and August) there were significant levels of SOC. The low correlation coefficient between OC and EC, especially during months with high levels of rainfall, such as April (Supplementary Fig. 5), signals that these species did not come from the same source. This suggests the presence of the secondary OC and the existence of mixed emission sources, including primary OC of biological origin, given that the sampling site is surrounded by green areas and is located ~250 m from the Botanical Garden of Bogotá. It is also possible that there were contributions to SOC from aged aerosols through long-range transport (Mancilla et al., 2015). A brief analysis of the correlation between OC/EC ratios and PM₁₀ levels is presented in Supplementary File (Fig. 6, p. 7).

3.5. Estimates of SOC

Differentiation between POC and SOC is relevant to analyze atmospheric aging processes of organic aerosols and to promote effective emission control policies. To calculate SOC, $(OC/EC)_{min}$ was first estimated for each of the sampled months. Based on this, monthly SOC was estimated (Eq. 1), resulting in values between 0.89 (August) and 2.73 (March). The annual value of SOC was calculated from the monthly average. An annual $(OC/EC)_{min}$ of 1.26 was obtained. This result was equivalent to that reported in urban background sites in Sao Paulo (1.03, Monteiro dos Santos et al., 2016) and Birmingham (1.0, Harrison et al., 2006), but higher than those in Madrid and Lisbon (0.55 for both, Pio et al., 2011), a finding which could be explained by the greater influence of diesel vehicles in European cities.

Monthly concentrations of POC and SOC are shown in Fig. 5. According to these results, during the study period POC contributed on average 55%, or $4.87 \mu\text{g}/\text{m}^3$, of total OC, whilst SOC contributed 45%, or $4.05 \mu\text{g}/\text{m}^3$, a figure that underlines the high impact of SOC on OC concentration in the study area.

The SOC concentrations at the sampling site were consistent with reports from other studies, which indicate that it is common to detect significant levels of secondary OC, in addition to primary OC, from fossil fuel combustion, in urban areas located at a reasonable distance from emission sources (Pio et al., 2011). The percentage of SOC was similar to findings in urban sites of large cities such as Baotou (37%–43%, Zhou et al., 2016) and Pune (47%, Safai et al., 2014), slightly higher than data from Sao Paulo (38%, Monteiro dos Santos et al., 2016) and lower than reports from Beijing (53%, Duan et al., 2005).

SOC concentrations ranged from $0.92 \mu\text{g}/\text{m}^3$ (July) to $6.05 \mu\text{g}/\text{m}^3$ (February) (Fig. 5). The highest concentrations were obtained between January and April, a period during which high levels of irradiance and the highest temperatures were registered (Table 1). The correlation coefficient between SOC and temperature ($R^2 = 0.61$, $P < 0.01$) (Supplementary Fig. 7) indicates a positive association between them, suggesting that SOC formation was higher during months with higher temperature as a result of photochemical activity (Castro et al., 1999). These results concur with those reported in other studies (Na et al., 2004; Pio et al., 2011; Safai et al., 2014), but disagree with others with respect to Chinese megacities (Ji et al., 2016; Wang et al., 2017) and some European cities (Lonati et al., 2007; Godec et al., 2016), where high SOC concentrations were noted in winter due to low temperatures accelerating the condensation of VOCs on particulate matter.

The data recorded from January to April suggests that high SOC levels could be related to high concentrations of precursor gases (NO₂ and SO₂) (Supplementary Table 5) and oxidizing agents (in the form of O₃ formed in the troposphere) (Alharbi et al., 2017; Zhong et al., 2017). The highest values of SOC (Fig. 5), O₃, NO₂ and SO₂ (Supplementary Table 5) were obtained when there were several forest fires, particularly in January and February. These compounds and VOCs concentrations have been associated with open biomass burning (Singh et al., 2015; Liu et al., 2017), revealing the high impact of forest fires on

SOC formation at the study site. Gasoline vehicles (> 2 million) have also been identified as the main source of VOCs in Bogotá (Franco et al., 2015), which coincides with the importance of secondary aerosol formation from gaseous precursors emitted by traffic found in other Latin American megacities (Vara-Vela et al., 2016). Although diesel vehicles do not dominate the traffic in the city, recent studies have reported their high contribution (as VOC and NO_x emitter) to SOC formation (Wei et al., 2017). Other possible contributors to SOC formation are the approximately 460,000 private gasoline motorcycles circulating in Bogotá (SDM, 2016), as these have been linked to elevated PAH and VOCs concentrations (Leong et al., 2002; Tsai et al., 2017), and biogenic VOCs, considering the characteristics of the sampling site described above. January and March reported the highest levels of solar radiation and temperature (Table 1), which may have coincided with a period of high biogenic VOC emissions.

The monthly SOC/OC ratios ranged from 0.16 (July) to 0.58 (May). Although this value varied during each month, a relatively stable pattern was observed during the study period (SOC/OC annual average = 0.44), suggesting that POC and SOC contributed to OC in similar proportions. However, the ratio was significantly lower (0.34 and 0.16, respectively) during June and July, which could be associated with favorable weather conditions for the dispersion of precursor gases, such as low levels of precipitation and high wind speeds (Table 1), preventing SOC formation. The results did not show a clear relationship between relative humidity and SOC formation processes as reported in other studies (Duan et al., 2005).

3.6. Effective carbon ratio (ECR)

Scattering and absorption properties are two crucial parameters in determining the impact of aerosol on the Earth's radiative balance. EC plays an important role in direct radiative forcing as a potential light-absorbing species (IPCC, 2015), and hence it is considered as the largest positive radiative force after carbon dioxide in inducing global warming (Jacobson, 2001; Bond et al., 2013). SOC generally scatters solar radiation (Pandis et al., 1992) and contributes to atmospheric cooling. The OC/EC ratio has been used to analyze the implications of aerosols for climate forcing (Novakov et al., 2005). Nevertheless, recent studies have found limitations to this methodology (because it does not offer information about carbonaceous aerosols sources) and have proposed calculating the ECR to obtain a better association between atmospheric carbonaceous particles and climate change (Safai et al., 2014; Pipal and Satsangi, 2015; Singh et al., 2015; Jia et al., 2016). The absorbing properties of POC (Lu et al., 2015) have been considered in the ECR, particularly those of brown carbon that increase sharply towards shorter wavelengths (Laskin et al., 2015). This is consistent with previous studies that have highlighted how most models tend to assume that organic aerosols are almost purely scattering, neglecting the light-absorbing properties of brown carbon (Lin et al., 2014). This species has been widely observed in biomass/biofuel and fossil fuel combustion sources, and several authors recommend including it in the climate contribution to improve aerosol light absorption analysis (Lu et al., 2015). Fig. 6 shows the monthly ECR values and the annual mean during the study period, which were calculated using Eq. 2 (Safai et al., 2014).

$$ECR = SOC/(POC + EC) \quad (2)$$

According to Safai et al. (2014), a higher ECR value indicates low POC and EC, which could suggest higher levels of direct radiative forcing and, consequently, a reduction in atmospheric warming effect of combustion aerosol. In our case, ECR values ranged between 0.74 (May) and 0.12 (July). Unlike the findings reported for other large cities, such as Pune and New Delhi (Pipal and Satsangi, 2015; Singh et al., 2015), no month registered an abundance of SOC compared to POC and EC ($ECR > 1.0$). ECR values > 0.6 were obtained in February, April and May (Fig. 6), during which higher concentrations of SOC than POC

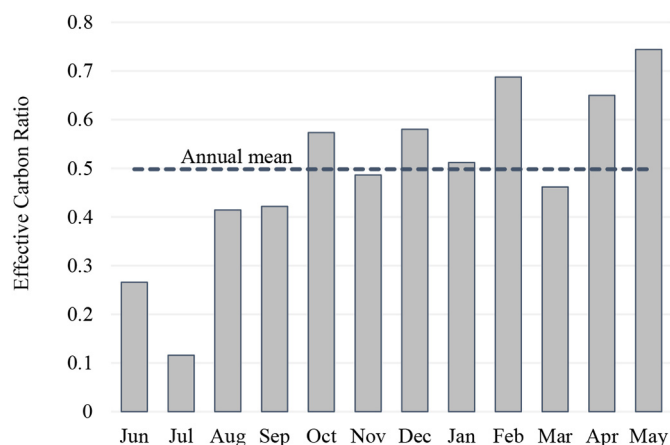


Fig. 6. ECR values during the study period.

were observed (Fig. 5). This indicates the predominance of scattering carbonaceous aerosols and a reduction in atmospheric warming. ECR values < 0.30 were obtained during June and July due to the lowest concentrations of SOC, suggesting a reduction in the number of scattering carbonaceous aerosols and possibly an increase in the absorbing type of carbonaceous aerosols. The annual mean was similar to that measured in urban areas in large Indian cities, such as Pune (0.55, Safai et al., 2014).

3.7. Air masses

Several studies have reported that SOC originates not only from local emissions but also from chemical transformation over regional and long-range transport (Schwarz et al., 2008; Sánchez De La Campa et al., 2009; Peng et al., 2016). Four clusters (sectors) were identified during the sampling period: i) east and northeast (E + NE), (ii) regional (R) (~100 km around the sampling point), (iii) south and southeast (S + SE), and iv) north (N) (Fig. 7).

According to the results, air masses coming from E + NE predominated during 62% of the sampled days, which is in line with what has been reported for Bogotá in previous studies (Ramírez, 2014). This sector included air masses coming from the northwest of Venezuela which crossed several departments of the Colombian Orinoquía Region, including Arauca, Casanare and Meta. This zone encompasses oil exploration and exploitation industries, is highly susceptible to forest fires, and registers biomass burning as an agricultural practice (Chacón, 2015), all of which are linked to high OC emissions and SOC precursor gases capable of spreading over regional areas and being transported over long distances (Simoneit, 2002). Fig. 7 shows that the days with an air mass domain of E + NE recorded the highest average OC concentrations ($9.66 \pm 4.84 \mu\text{g}/\text{m}^3$). January 14 and February 2–3 registered the highest OC concentrations of the whole year (between $19 \mu\text{g}/\text{m}^3$ and $24 \mu\text{g}/\text{m}^3$). On these days air masses arrived at the sampling site from the east and northeast. Hence, the high OC concentrations during January and February (Fig. 2), when winds from NE–E–SE predominated (Supplementary Fig. 1), could be explained by both the aforementioned local emissions and by long distance SOC contributions. An example of a day on which the prevailing air mass was from E + NE (February 07, 2016) is shown in Supplementary Fig. 8.

Regional air masses and winds from S + SE were less frequent (19% and 18% of the sampling period, respectively). Air masses from S + SE included winds blowing from the Amazon region of Ecuador, Brazil, Venezuela and Colombia, as well as from the south of the department of Meta, where forest fires and biomass burning were reported as agricultural practices during the sampling period. Winds from S + SE were present, particularly on some days of August, September and May, which coincided with the dry season in the Amazon region (May to

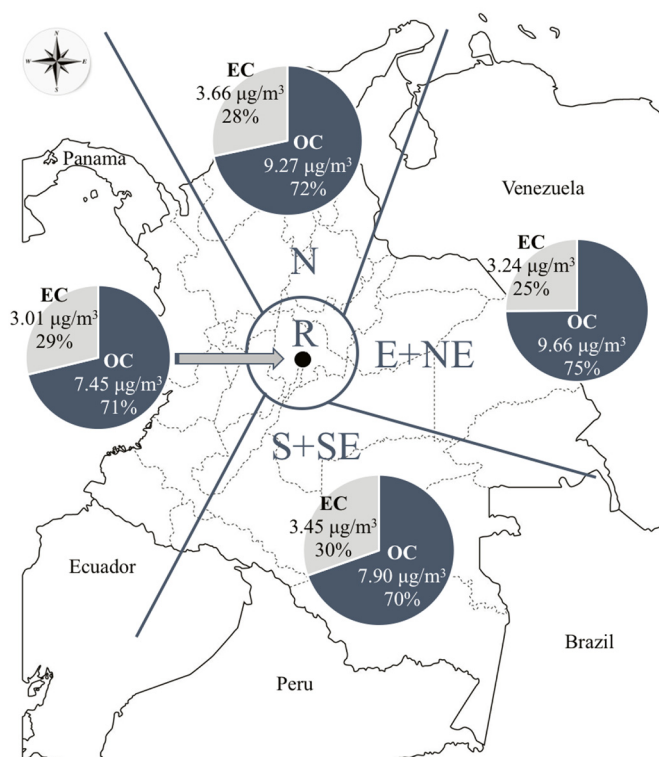


Fig. 7. OC and EC concentrations according to back-trajectories cluster. Examples of each sector are shown in Supplementary Fig. 8.

September) (Pivello, 2011). This means that OC contributions from Amazonian fires could happen during this period in the study area. Finally, air masses from N were registered 1% of the time (4 days), especially during the first days of November. Supplementary Fig. 8 shows examples of back-trajectories of regional (September 24, 2015), S + SE (August 15, 2015) and N origin (November 03, 2015).

4. Conclusions

This study analyzed the characteristics and the temporal variability of the carbonaceous fraction on PM_{10} , from daily samples collected during an El Niño year at an urban background site in a tropical, high-altitude megacity.

Our analyses revealed that the months with the highest mean OC values were January, February and March, which were characterized by high temperatures and significant levels of irradiance. The chief natural source of OC during this period was forest fires, while anthropogenic sources of OC, such as traffic and industrial activities, predominated the rest of the year. The high degree of variability in OC concentrations were linked to meteorological conditions, urban dynamics and long-distance contributions during the sampling period. On the other hand, EC concentrations were relatively constant throughout the year, and its origin was mainly related to local combustion processes located to the west of the city, such as industrial emissions, diesel trucks and bus traffic. However, months with high rainfall levels (November and April) registered higher concentrations of EC. Forest fires were also identified as a relevant source of EC in the dry period. Additionally, the results suggested that the concentration of carbonaceous aerosols was ~35% higher on weekdays than on weekends. The high impact of SOC in OC concentration was evidenced in the study area. The peak concentrations of SOC were measured in the months with the highest temperature, indicating their photochemical origin. According to ECR results, the presence of scattering carbonaceous aerosols predominated during the study period. This study revealed that, at the local level, winds from the West (affected by industrial and vehicular emissions) increased

concentrations of carbonaceous species at the sampling site. At the regional level, air masses from the E + NE (crossing Venezuela and Colombia's Eastern Plains) increased OC concentrations, as a result of long distance SOC contributions.

From a critical perspective, a better knowledge of the characteristics and temporal variation of organic compounds would be achieved with an analysis of the organic chemical composition of PM₁₀. This would enrich the results of our work. It is also advisable to replicate this study in other sites of Bogota, which would allow to obtain a clearer picture of the entire city. On the other hand, it is recommended to sample during a year with a predominance of La Niña phenomenon, which presents very different meteorological conditions from those of El Niño phenomenon. This would yield new data on the variability of OC, EC and TC during extreme weather events, their sources and effects on climate change.

Acknowledgments

Thanks to Universidad Internacional de Andalucía–UNIA, to the Regional Council for the Environment of Junta de Andalucía, and to Universidad Nacional Abierta y a Distancia–UNAD for partially funding this project. Thanks also to the NOAA Air Resources Laboratory (ARL) for providing the HYSPLIT transport and dispersion model, and to the District Secretary of the Environment, Bogota (SDA) for meteorological and air quality data. Finally, thanks to Diana Ramírez (Monash University) for her comments.

Appendix A. Supplementary data

Supplementary data to this article can be found online at <https://doi.org/10.1016/j.atmosres.2018.04.006>.

References

- Aiken, A., Decarlo, P., Kroll, J., Worsnop, D., Huffman, J., Docherty, K., Ulbrich, I., Mohr, C., Kimmel, J., Sueper, D., Sun, Y., Zhang, Q., Trimborn, A., Northway, M., Ziemann, P., Canagaratna, M., Onasch, T., Alfarra, M., Prevot, A., Dommen, J., Duplissy, J., Metzger, A., Baltensperger, U., Jimenez, J., 2008. O/C and OM/OC ratios of primary, secondary, and ambient organic aerosols with high-resolution time-of-flight aerosol mass spectrometry. *Environ. Sci. Technol.* 42 (12), 4478–4485.
- Alharbi, B., Alduwais, A., Alhuthodi, A., 2017. An analysis of the spatial distribution of O₃ and its precursors during summer in the urban atmosphere of Riyadh, Saudi Arabia. *Atmos. Pollut. Res.* 8, 861–872.
- Alves, A., Oliveira, C., Martins, N., Mirante, F., Caseiro, A., Pio, C., Matos, M., Silva, H., Oliveira, C., Camões, F., 2016. Road tunnel, roadside, and urban background measurements of aliphatic compounds in size-segregated particulate matter. *Atmos. Res.* 168, 139–148.
- Birch, M., Cary, R., 1996. Elemental carbon-based method for monitoring occupational exposures to particulate diesel exhaust. *Aerosol Sci. Technol.* 25 (3), 221–241.
- Bisht, D., Dumka, U., Kaskaoutis, D., Pipal, A., Srivastava, A., Soni, V., Attri, S., Sateesh, M., Tiwari, S., 2015. Carbonaceous aerosols and pollutants over Delhi urban environment: temporal evolution, source apportionment and radiative forcing. *Sci. Total Environ.* 521–522, 431–445.
- Bond, T., Doherty, S., Fahey, D., Forster, P., Bernsten, T., Deangelo, B., Flanner, M., Ghan, S., Kärcher, B., Koch, D., Kinne, S., Kondo, Y., Quinn, P., Sarofim, M., Schultz, M., Schulz, M., Venkataraman, C., Zhang, H., Zhang, S., Bellouin, N., Guttikunda, S., Hopke, P., Jacobson, M., Kaiser, J., Klimont, Z., Lohmann, U., Schwarz, J., Shindell, D., Storelvmo, T., Warren, S., Zender, C., 2013. Bounding the role of black carbon in the climate system: a scientific assessment. *J. Geophys. Res. Atmos.* 118, 5380–5552.
- Bravo, H., Sosa, R., Sanchez, P., Krupa, S., 2013. Air quality standards for particulate matter (PM) at high altitude cities. *Environ. Pollut.* 173, 255–256.
- Brito, J., Rizzo, L., Herckes, P., Vasconcellos, P., Caumo, S., Fornaro, A., Ynoue, R., Artaxo, P., Andrade, M., 2013. Physical–chemical characterisation of the particulate matter inside two road tunnels in the Sao Paulo Metropolitan Area. *Atmos. Chem. Phys.* 13, 12199–12213.
- Carmona, L., Rincón, M., Castillo, A., Galvis, B., Sáenz, H., Manrique, R., Pachón, P., 2016. Conciliación de inventarios top-down y bottom-up de emisiones de fuentes móviles en Bogotá, Colombia. *Tecnica* 20 (49), 59–74.
- Castro, L., Pio, C., Harrison, R., Smith, D., 1999. Carbonaceous aerosol in urban and rural European atmospheres: estimation of secondary organic carbon concentrations. *Atmos. Environ.* 33, 2771–2781.
- Cavalli, F., Viana, M., Yttri, K., Genberg, J., Putaud, J., 2010. Toward a standardised thermal–optical protocol for measuring atmospheric organic and elemental carbon: the EUSAAR protocol. *Atmos. Meas. Tech.* 3, 79–89.
- Chacón, L., 2015. Efecto de los Incendios forestales sobre la calidad del aire en dos ciudades colombianas. Tesis de Maestría en Ingeniería Ambiental. Universidad Nacional de Colombia, Bogotá.
- Chameides, W., Bergin, M., 2002. Climate change. Soot takes center stage. *Science* 297, 2214–2215.
- Chen, X., Yu, J., 2007. Measurement of organic mass to organic carbon ratio in ambient aerosol samples using a gravimetric technique in combination with chemical analysis. *Atmos. Environ.* 41, 8857–8864.
- Chow, J., Watson, J., Fujita, E., Lu, Z., Lawson, D., 1994. Temporal and spatial variations of PM_{2.5} and PM₁₀ aerosol in the southern California air quality study. *Atmos. Environ.* 28 (12), 2061–2080.
- Chow, J., Watson, J., Lu, Z., Lowenthal, D., Frazier, C., Solomon, P., Thuillier, R., Magliano, K., 1996. Descriptive analysis of PM_{2.5} and PM₁₀ at regionally representative locations during SJAQS/AUSPEX. *Atmos. Environ.* 30, 2079–2112.
- Chung, C., Ramanathan, V., Decremet, D., 2012. Observationally constrained estimates of carbonaceous aerosol radiative forcing. *Proc. Natl. Acad. Sci. U. S. A.* 109, 11624–11629.
- Custódio, D., Cerqueira, M., Fialho, P., Nunes, T., Pio, C., Henriques, D., 2014. Wet deposition of particulate carbon to the Central North Atlantic Ocean. *Sci. Total Environ.* 496, 92–99. <http://dx.doi.org/10.1016/j.scitotenv.2014.06.103>.
- DANE, 2010. Proyecciones Nacionales y Departamentales de Población 2005–2020. DANE, Bogotá.
- De Oliveira, N., Brito, J., Caumo, S., Arana, A., De Souza, S., Artaxo, P., Hillamo, R., Teinila, K., De Medeiros, S., De Castro, P., 2015. Biomass burning in the Amazon region: aerosol source apportionment and associated health risk assessment. *Atmos. Environ.* 120, 277–285.
- DeCarlo, P., Ulbrich, I., Crounse, J., de Foy, B., Dunlea, E., Aiken, A., Knapp, D., Weinheimer, A., Campos, T., Wennberg, P., Jimenez, J., 2010. Investigation of the sources and processing of organic aerosol over the Central Mexican Plateau from aircraft measurements during MILAGRO. *Atmos. Chem. Phys.* 10, 5257–5280.
- Demographia, 2017. Demographia world urban areas. 13th annual edition. <http://demographia.com/db-worldua.pdf> (accessed 29 June 2017).
- Didyk, B., Simoneit, B., Pezosa, L., Riveros, M., Flores, A., 2000. Urban aerosol particles of Santiago, Chile: organic content and molecular characterization. *Atmos. Environ.* 34, 1167–1179.
- Duan, F., He, K., Ma, Y., Jia, Y., Yang, F., Lei, Y., Tanaka, S., Okuta, T., 2005. Characteristics of carbonaceous aerosols in Beijing, China. *Chemosphere* 60, 355–364.
- El-Zanan, H., Zielinska, B., Mazzoleni, L., Hansen, D., 2009. Analytical determination of the aerosol organic mass-to-organic carbon ratio. *J. Air Waste Manage. Assoc.* 59 (1), 58–69.
- Escudero, M., Viana, M., Querol, X., Alastuey, A., Díez Hernández, P., García Dos Santos, S., Anzano, J., 2015. Industrial sources of primary and secondary organic aerosols in two urban environments in Spain. *Environ. Sci. Pollut. Res.* 22, 10413–10424.
- Fang, G., Wu, Y., Chou, T., Lee, Ch., 2008. Organic carbon and elemental carbon in Asia: a review from 1996 to 2006. *J. Hazard. Mater.* 150, 231–237.
- Feng, X., Wang, Sh., 2012. Influence of different weather events on concentrations of particulate matter with different sizes in Lanzhou, China. *J. Environ. Sci.* 24 (4), 665–674.
- Feng, Y., Chen, Y., Guo, H., Zhi, G., Xiong, S., Li, J., Sheng, G., Fu, J., 2009. Characteristics of organic and elemental carbon in PM_{2.5} samples in Shanghai, China. *Atmos. Res.* 92 (4), 434–442.
- Franco, J., Belalcázar, L., Behrentz, E., 2015. Characterization and source identification of VOC species in Bogotá, Colombia. *Atmósfera* 28 (1), 1–11.
- Franco, J., Segura, J., Mura, I., 2016. Air pollution alongside bike-paths in Bogotá–Colombia. *Front. Environ. Sci.* 4, 77. <http://dx.doi.org/10.3389/fenvs.2016.00077>.
- Fuzzi, S., Andrea, M., Huebert, B., Kulmala, M., Bond, T., Boy, M., Doherty, S., Guenther, A., Kanakidou, M., Kawamura, K., Kerminen, V., Lohmann, U., Russell, L., Poeschl, U., 2006. Critical assessment of the current state of scientific knowledge, terminology, and research needs concerning the role of organic aerosols in the atmosphere, climate, and global change. *Atmos. Chem. Phys.* 6, 2017–2038.
- Gelencsér, A., May, B., Simpson, D., Sánchez-Ochoa, A., Kasper-Giebl, A., Puxbaum, H., Caseiro, A., Pio, C., Legrand, M., 2007. Source apportionment of PM_{2.5} organic aerosol over Europe: primary/secondary, natural/anthropogenic, and fossil/biogenic origin. *J. Geophys. Res. Atmos.* 112, D23S04. <http://dx.doi.org/10.1029/2006JD008094>.
- Godec, R., Jakovljevic, I., Segal, K., Cackovic, M., Beslic, I., Davila, S., Pehnec, G., 2016. Carbon species in PM₁₀ particle fraction at different monitoring sites. *Environ. Pollut.* 216, 700–710.
- Green, J., Sánchez, S., 2013. Air Quality in Latin America: An Overview. Clean Air Institute, Washington D.C.
- Grivas, G., Cheristanidis, S., Chaloulakou, A., 2012. Elemental and organic carbon in the urban environment of Athens. Seasonal and diurnal variations and estimates of secondary organic carbon. *Sci. Total Environ.* 414, 535–545.
- Gulia, S., Nagendra, S., Khare, M., Khanna, I., 2015. Urban air quality management – a review. *Atmos. Pollut. Res.* 6, 286–304.
- Guo, L., Zhang, Y., Lin, H., Zeng, W., Liu, T., Xiao, J., Rutherford, Sh., You, J., Ma, W., 2016. The washout effects of rainfall on atmospheric particulate pollution in two Chinese cities. *Environ. Pollut.* 215, 195–202.
- Han, Y., Chen, L., Huang, R., Chow, J., Watson, J., Ni, H., Liu, S., Fung, K., Shen, Z., Wei, C., Wang, Q., Tian, J., Zhao, Z., Prévôt, A., Cao, J., 2016. Carbonaceous aerosols in megacity Xi'an, China: implications of thermal/optical protocols comparison. *Atmos. Environ.* 132, 58–68.
- Harrison, R., Jones, A., Lawrence, R., 2004. Major component composition of PM₁₀ and PM_{2.5} from roadside and urban background sites. *Atmos. Environ.* 38, 4531–4538.
- Harrison, R., Yin, Y., Tilling, R., Cai, X., Seakins, P., Hopkins, J., Lansley, D., Lewis, A.,

- Hunter, M., Heard, D., Carpenter, L., Creasey, D., Lee, J., Pilling, M., Carslaw, N., Emmerson, K., Redington, A., Derwent, R., Ryall, D., Mills, G., Penkett, S., 2006. Measurement and modelling of air pollution and atmospheric chemistry in the U.K. West Midlands conurbation: overview of the PUMA consortium project. *Sci. Total Environ.* 360, 5–25.
- Hitzenberger, R., Ctyroky, P., Berner, A., Tursic, J., Podkrajsek, B., Grgic, I., 2006. Size distribution of black (BC) and total carbon (TC) in Vienna and Ljubljana. *Chemosphere* 65, 2106–2113.
- Ho, K., Lee, S., Chan, Ch., Yu, J., Chow, J., Yao, X., 2003. Characterization of chemical species in PM_{2.5} and PM₁₀ aerosols in Hong Kong. *Atmos. Environ.* 37, 31–39.
- Huang, X., Yu, J., 2008. Size distributions of elemental carbon in the atmosphere of a coastal urban area in South China: characteristics, evolution processes, and implications for the mixing state. *Atmospheric Chem. Phys.* 8, 5843–5853.
- IDEAM, 2014. Evolución de precipitación y temperatura durante los fenómenos El niño y La Niña en Bogotá – Cundinamarca (1951–2012). IDEAM/PNUD, Bogotá.
- IDEAM, 2015a. Atlas climatológico de Colombia – Interactivo. <http://atlas.ideam.gov.co/visorAtlasClimatologico.html>, Accessed date: 9 November 2016.
- IDEAM, 2015b. Atlas de vientos de Colombia – Interactivo. <http://atlas.ideam.gov.co/visorAtlasVientos.html>, Accessed date: 9 November 2016.
- IDEAM, 2016. Informe del estado de la calidad del aire en Colombia, 2011–2015. DANE, Bogotá.
- IHME, 2017. State of Global Air. A special report on global exposure to air pollution and its disease burden. Health Effects Institute, Boston.
- IPCC, Pachauri, R.K., Meyer, L.A., 2015. In: Team, Core Writing (Ed.), *Climate Change 2014: Synthesis Report. Contribution of Working Groups I, II and III to the Fifth Assessment Report of the Intergovernmental Panel on Climate Change*. IPCC, Geneva.
- Jacobson, M., 2001. Strong radiative heating due to the mixing state of black carbon in atmospheric aerosols. *Nature* 409, 695–697.
- Ji, D., Zhang, J., He, J., Wang, X., Pang, B., Liu, Z., Wang, L., Wang, Y., 2016. Characteristics of atmospheric organic and elemental carbon aerosols in urban Beijing, China. *Atmos. Environ.* 125, 293–306.
- Jia, H., Wang, L., Li, P., Wang, Y., Guo, L., Li, T., Sun, L., Shou, Y., Mao, T., Yi, X., 2016. Characterization, long-range transport and source identification of carbonaceous aerosols during spring and autumn periods at a High Mountain site in South China. *Atmosphere* 7 (10), 122. <http://dx.doi.org/10.3390/atmos7100122>.
- Keller, A., Bartscher, H., 2017. Characterizing particulate emissions from wood burning appliances including secondary organic aerosol formation potential. *J. Aerosol Sci.* 114, 21–30. <http://dx.doi.org/10.1016/j.jaerosci.2017.08.014>.
- Khan, M., Masiol, M., Formenton, G., Di Gilio, A., de Gennaro, G., Agostinelli, C., Pavoni, B., 2016. Carbonaceous PM_{2.5} and secondary organic aerosol across the Veneto region (NE Italy). *Sci. Total Environ.* 542, 172–181.
- Kroll, J., Seinfeld, J., 2008. Chemistry of secondary organic aerosol: formation and evolution of low-volatility organics in the atmosphere. *Atmos. Environ.* 42 (16), 3593–3624. <http://dx.doi.org/10.1016/j.atmosenv.2008.01.003>.
- Laskin, A., Laskin, J., Nizkorodov, S., 2015. Chemistry of atmospheric brown carbon. *Chem. Rev.* 115, 4335–4382. <http://dx.doi.org/10.1021/cr5006167>.
- Leong, Sh., Muttamara, S., Laortanakul, P., 2002. Influence of benzene emission from motorcycle on Bangkok air quality. *Atmos. Environ.* 36 (4), 651–661.
- Lin, J., Tai, H., 2001. Concentrations and distributions of carbonaceous species in ambient particles in Kaohsiung City, Taiwan. *Atmos. Environ.* 35, 2627–2636.
- Lin, G., Penner, J., Flanner, M., Sillman, S., Xu, L., Zhou, Ch., 2014. Radiative forcing of organic aerosol in the atmosphere and on snow: effects of SOA and brown carbon. *J. Geophys. Res. Atmos.* 119, 7453–7476. <http://dx.doi.org/10.1002/2013JD021186>.
- Liu, X., Huey, L., Yokelson, R., Selimovic, V., Simpson, I., Müller, M., Jimenez, J., Campuzano-Jost, P., Beyersdorf, A., Blake, D., Butterfield, Z., Choi, Y., Crounse, J., Day, D., Diskin, G., Dubey, M., Fortner, E., Hanisco, T., Hu, W., King, L., Kleinman, L., Meinardi, S., Mikoviny, T., Onasch, T., Palm, B., Peischl, J., Pollack, I., Ryerson, T., Sachse, G., Sedlacek, A., Shilling, J., Springston, S., St. Clair, J., Tanner, D., Teng, A., Wennberg, P., Wisthaler, A., Wolfe, G., 2017. Airborne measurements of western U.S. wildfire emissions: Comparison with prescribed burning and air quality implications. *J. Geophys. Res. Atmos.* 122. <http://dx.doi.org/10.1002/2016JD026315>.
- Lonati, G., Ozgen, S., Giugliano, M., 2007. Primary and secondary carbonaceous species in PM_{2.5} samples in Milan (Italy). *Atmos. Environ.* 41, 4599–4610.
- Lu, Z., Streets, D., Winijkul, E., Yan, F., Chen, Y., Bond, T., Feng, Y., Dubey, M., Liu, Sh., Pinto, J., Carmichael, G., 2015. Light absorption properties and radiative effects of primary organic aerosol emissions. *Environ. Sci. Technol.* 49, 4868–4877. <http://dx.doi.org/10.1021/acs.est.5b00211>.
- Mancilla, Y., Herckes, P., Fraser, M., Mendoza, A., 2015. Secondary organic aerosol contributions to PM_{2.5} in Monterrey, Mexico: temporal and seasonal variation. *Atmos. Res.* 153, 348–359.
- Mauderly, J., Chow, J., 2008. Health effects of organic aerosols. *Inhal. Toxicol.* 20 (3), 257–288.
- Mkoma, S., Maenhaut, W., Chi, X., Wang, W., Raes, N., 2009. Characterisation of PM₁₀ atmospheric aerosols for the wet season 2005 at two sites in East Africa. *Atmos. Environ.* 43, 631–639.
- Molina, L., Molina, M., Slott, R., Kolb, C., Gbor, P., Meng, F., Singh, R., Galvez, O., Sloan, J., Anderson, W., Tang, X., Shao, M., Zhu, T., Zhang, Y., Hu, M., Gurjar, B., Artaxo, P., Oyola, P., Gramsch, E., Hidalgo, P., Gertler, A., 2004a. Air quality in selected megacities. *J. Air Waste Manag. Assoc.* 54 (12), 1–73.
- Molina, M., Ivanov, A., Trakhtenberg, S., Molina, L., 2004b. Atmospheric evolution of organic aerosol. *Geophys. Res. Lett.* 31, L22104. <http://dx.doi.org/10.1029/2004GL020910>.
- Monteiro dos Santos, D., Brito, J., Godoy, J., Artaxo, P., 2016. Ambient concentrations and insights on organic and elemental carbon dynamics in Sao Paulo, Brazil. *Atmos. Environ.* 144, 226–233.
- Mugica, V., Ortiz, E., Molina, L., de Vizcaya-Ruiz, A., Nebot, A., Quintana, R., Aguilar, J., Alcántara, E., 2009. PM composition and source reconciliation in Mexico City. *Atmos. Environ.* 43, 5068–5074.
- Na, K., Sawant, A., Song, Ch., Cocker III, D., 2004. Primary and secondary carbonaceous species in the atmosphere of Western Riverside County, California. *Atmos. Environ.* 38, 1345–1355.
- Novakov, T., Menon, S., Kirchstetter, T., 2005. Aerosol organic carbon to black carbon ratios: analysis of published data and implications for climate forcing. *J. Geophys. Res.* 110, D21205. <http://dx.doi.org/10.1029/2005JD005977>.
- Pandis, S., Harley, R., Cass, G., Seinfeld, J., 1992. Secondary organic aerosol formation and transport. *Atmos. Environ.* 26 (13), 2269–2282.
- Peng, J., Hu, M., Gong, Z., Tian, X., Wang, M., Zheng, J., Guo, Q., Cao, W., Lv, W., Hu, W., Wu, Z., Guo, S., 2016. Evolution of secondary inorganic and organic aerosols during transport: a case study at a regional receptor site. *Environ. Pollut.* 218, 794–803.
- Philip, S., Martin, R., Pierce, J., Jimenez, J., Zhang, Q., Canagaratna, M., Spracklen, D., Nowlan, C., Lamsal, L., Cooper, M., Krotkov, N., 2014. Spatially and seasonally resolved estimate of the ratio of organic mass to organic carbon. *Atmos. Environ.* 87, 34–40.
- Pio, C., Cerqueira, M., Harrison, R., Nunes, T., Mirante, F., Alves, C., Oliveira, C., Sánchez de la Campa, A., Artiñano, B., Matos, M., 2011. OC/EC ratio observations in Europe: re-thinking the approach for apportionment between primary and secondary organic carbon. *Atmos. Environ.* 45, 6121–6132.
- Pipal, A., Satsangi, G., 2015. Study of carbonaceous species, morphology and sources of fine (PM_{2.5}) and coarse (PM₁₀) particles along with their climatic nature in India. *Atmos. Res.* 154, 103–115.
- Pivello, V., 2011. The use of fire in the Cerrado and Amazonian rainforests of Brazil: past and present. *Fire Ecol.* 7 (1), 24–39. <http://dx.doi.org/10.4996/fireecology.0701024>.
- Querol, X., Alastuey, A., Ruiz, C., Artiñano, B., Hansson, H., Harrison, R., Buringh, E., ten Brink, H., Lutz, M., Bruckmann, P., Straehl, P., Schneider, J., 2004. Speciation and origin of PM₁₀ and PM_{2.5} in selected European cities. *Atmos. Environ.* 38, 6547–6555.
- Ramírez, O., 2014. Origen de masas de aire en cuatro ciudades de Colombia mediante el modelo HYSPLIT. *Revista de Investigación Agraria y Ambiental* 5 (1), 103–119.
- Ramírez, O., Sánchez de la Campa, A.M., Amato, F., Catacolí, R., Rojas, N., de la Rosa, J., 2018. Chemical composition and source apportionment of PM₁₀ at an urban background site in a high-altitude Latin American megacity (Bogotá, Colombia). *Environ. Pollut.* 233, 142–155.
- Rolph, G., Stein, A., Stunder, B., 2017. Real-time environmental applications and display system: READY. *Environ. Model. Softw.* 95, 210–228.
- Sánchez Campa De La, A., Pio, C., de la Rosa, J., Querol, X., Alastuey, A., González-Castanedo, Y., 2009. Characterization and origin of EC and OC particulate matter near the Doñana National Park (SW Spain). *Environ. Res.* 109, 671–681.
- Safai, P., Raju, M., Rao, P., Pandithurai, G., 2014. Characterization of carbonaceous aerosols over the urban tropical location and a new approach to evaluate their climatic importance. *Atmos. Environ.* 92, 493–500.
- Salma, I., Chi, X., Maenhaut, W., 2004. Elemental and organic carbon in urban canyon and background environments in Budapest, Hungary. *Atmos. Environ.* 38, 27–36.
- Samara, C., Voutsas, D., Kouras, A., Eleftheriadis, K., Maggos, T., Saraga, D., Petrakakis, M., 2014. Organic and elemental carbon associated to PM₁₀ and PM_{2.5} at urban sites of northern Greece. *Environ. Sci. Pollut. Res.* 21, 1769–1785.
- Schwarz, J., Chi, X., Maenhaut, W., Civiš, M., Hovorka, J., Smolík, J., 2008. Elemental and organic carbon in atmospheric aerosols at downtown and suburban sites in Prague. *Atmos. Res.* 90, 287–302.
- SDA, 2009. Elementos Técnicos del Plan Decenal de Descontaminación de Bogotá. In: Parte 2: Inventario de Emisiones Provenientes de Fuentes Fijas y Móviles. Alcaldía Mayor de Bogotá/Universidad de Los Andes, Bogotá.
- SDA, 2015. Informe anual de calidad del aire de Bogotá, 2014. SDA/Alcaldía Mayor de Bogotá, Bogotá.
- SDA, 2016. Informe anual de calidad del aire de Bogotá, 2015. SDA/Alcaldía Mayor de Bogotá, Bogotá.
- SDA, 2017. Informe anual de calidad del aire de Bogotá, 2016. SDA/Alcaldía Mayor de Bogotá, Bogotá.
- SDM, 2016. Observatorio Ambiental de Bogotá. Bogotá, Secretaría Distrital de Ambiente – SDA. <http://oab.ambienteBogota.gov.co/es/temas?v=6&p=21>, Accessed date: 4 June 2017.
- Seguel, S., Morales, R., Leiva, M., 2009. Estimations of primary and secondary organic carbon formation in PM_{2.5} aerosols of Santiago City, Chile. *Atmos. Environ.* 43, 2125–2131.
- Segura, J., Franco, J., 2016. Exposición de peatones a la contaminación del aire en vías con alto tráfico vehicular. *Rev. salud pública* 18 (2), 179–187.
- Simoneit, B., 2002. Biomass burning – a review of organic tracers for smoke from incomplete combustion. *Appl. Geochem.* 17, 129–162.
- Singh, R., Kulshrestha, M., Kumar, B., Chandra, S., 2015. Impact of anthropogenic emissions and open biomass burning on carbonaceous aerosols in urban and rural environments of Indo-Gangetic Plain. *Air Qual. Atmos. Health* 9 (7), 809–822.
- Slinn, W., 1984. Precipitation scavenging. In: Randerson, D. (Ed.), *Atmospheric Sciences and Power Production*. U.S. Department of Energy, Washington, D.C.
- Stein, A., Draxler, R., Rolph, G., Stunder, B., Cohen, M., Ngan, F., 2015. NOAA's Hysplit atmospheric transport and dispersion modeling system. *Bull. Am. Meteorol. Soc.* 96 (12), 2059–2077.
- Terzi, E., Argyropoulos, G., Bougiatioti, A., Mihalopoulos, N., Nikolaou, K., Samara, C., 2010. Chemical composition and mass closure of ambient PM₁₀ at urban sites. *Atmos. Environ.* 44, 2231–2239.
- Tritscher, T., Jurányi, Z., Martin, M., Chirico, R., Gysel, M., Heringa, M.F., DeCarlo, P., Sierau, B., Prevot, A., Weingartner, E., Baltensperger, U., 2011. Changes of hygroscopicity and morphology during ageing of diesel soot. *Environ. Res. Lett.* 6, 034026. <http://dx.doi.org/10.1088/1748-9326/6/3/034026>.
- Tsai, J., Huang, P., Chiang, H., 2017. Air pollutants and toxic emissions of various mileage

- motorcycles for ECE driving cycles. *Atmos. Environ.* 153, 126–134.
- UNEP, 2016. Global Environment Outlook (GEO-6). Regional Assessment for Latin America and the Caribbean. United Nations Environment Programme, Nairobi.
- US EPA, 1999. Sampling of Ambient Air for Suspended Particle Matter (SPM) and PM₁₀ Using High Volume (HV) Sampler. Method IO-2.1.
- Vara-Vela, A., Andrade, M., Kumar, P., Ynoue, R., Muñoz, A., 2016. Impact of vehicular emissions on the formation of fine particles in the Sao Paulo Metropolitan Area: a numerical study with the WRF-Chem model. *Atmos. Chem. Phys.* 16, 777–797.
- Vargas, F., Rojas, N., Pachón, J., Russell, A., 2012. PM₁₀ characterization and source apportionment at two residential areas in Bogota. *Atmos. Pollut. Res.* 3, 72–80.
- Vasconcellos, P., Souza, D., Ávila, S., Araújo, M., Naoto, E., Nascimento, K., Cavalcante, F., Dos Santos, M., Smichowski, P., Behrentz, E., 2011. Comparative study of the atmospheric chemical composition of three South American cities. *Atmos. Environ.* 45, 5770–5777.
- Viana, M., Chi, X., Maenhaut, W., Cafmeyer, J., Querol, X., Alastuey, A., Mikuska, P., Vecera, Z., 2006. Influence of sampling artefacts on measured PM, OC and EC levels in carbonaceous aerosols in an urban area. *Aerosol Sci. Technol.* 40 (2), 107–117.
- Wang, Q., Jiang, N., Yin, Sh., Li, X., Yu, F., Guo, Y., Zhang, R., 2017. Carbonaceous species in PM_{2.5} and PM₁₀ in urban area of Zhengzhou in China: seasonal variations and source apportionment. *Atmos. Res.* 191, 1–11.
- Wei, D., Qihou, H., Tengyu, L., Xinming, W., Yanli, Z., Wei, S., Yele, S., Xinhui, B., Jianzhen, Y., Weiqiang, Y., Xinyu, H., Zhou, Z., Zhonghui, H., Quanfu, H., Mellouki, A., George, C., 2017. Primary particulate emissions and secondary organic aerosol (SOA) formation from idling diesel vehicle exhaust in China. *Sci. Total Environ.* 593–594, 462–469.
- WHO, 2006. WHO Air Quality Guidelines for Particulate Matter, Ozone, Nitrogen Dioxide and Sulfur Dioxide. WHO, Geneva.
- WHO, 2012. Health Effects of Black Carbon. WHO's Regional Office for Europe, Copenhagen.
- WHO, 2016. World Health Statistics 2016. WHO, Geneva.
- Wu, G., Du, X., Wu, X., Fu, X., Kong, Sh., Chen, J., Wang, Z., Bai, Z., 2013. Chemical composition, mass closure and sources of atmospheric PM₁₀ from industrial sites in Shenzhen, China. *J. Environ. Sci.* 25 (8), 1626–1635.
- Xu, L., Chen, X., Chen, J., Zhang, F., He, Ch., Du, K., Wang, Y., 2012. Characterization of PM₁₀ atmospheric aerosol at urban and urban background sites in Fuzhou city, China. *Environ. Sci. Pollut. Res.* 19, 1443–1453.
- Yin, J., Harrison, R., 2008. Pragmatic mass closure study for PM_{1.0}, PM_{2.5} and PM₁₀ at roadside, urban background and rural sites. *Atmos. Environ.* 42, 980–988.
- Yuan, Z., 2014. The effect of rains of different intensity on mass concentration of PM_{2.5} in Dongguan City. *Guangdong Meteorol.* 36, 32–35.
- Zhang, Y., Schauer, J.J., Zhang, Y., Zeng, L., Wei, Y., Liu, Y., Shao, M., 2008. Characteristics of particulate carbon emissions from real-world Chinese coal combustion. *Environ. Sci. Technol.* 42, 5068–5073.
- Zhong, J., Cai, X., Bloss, W., 2017. Large eddy simulation of reactive pollutants in a deep urban street canyon: coupling dynamics with O₃–NO_x–VOC chemistry. *Environ. Pollut.* 224, 171–184.
- Zhou, H., He, J., Zhao, B., Zhang, L., Fan, Q., Lü, Ch., Liu, T., Yuan, Y., 2016. The distribution of PM₁₀ and PM_{2.5} carbonaceous aerosol in Baotou, China. *Atmos. Res.* 178–179, 102–113.
- Zhu, T., Melamed, M., Parrish, D., Gauss, M., Gallardo, L., Lawrence, M., Konare, A., Lioussé, C., 2012. Impacts of Megacities on Air Pollution and Climate. WMO/IGAC, Geneva.